The Company of Biologists

RESEARCH ARTICLE

Sensing the structural characteristics of surfaces: texture encoding by a bottom-dwelling fish

Adam R. Hardy and Melina E. Hale*

ABSTRACT

The texture of contacted surfaces influences our perception of the physical environment and modulates behavior. Texture perception and its neural encoding mechanisms have traditionally been studied in the primate hand, yet animals of all types live in richly textured environments and regularly interact with textured surfaces. Here we explore texture sensation in a different type of vertebrate limb by investigating touch and potential texture encoding mechanisms in the pectoral fins of fishes, the forelimb homologs. We investigated the pectoral fins of the round goby (*Neogobius melanostomus*), a bottom-dwelling species that lives on substrate types of varying roughness and whose fins frequently contact the bottom. Analysis shows that the receptive field sizes of fin ray afferents are small and afferents exhibit response properties to tactile motion that are consistent with those of primates and other animals studied previously. In response to a periodic stimulus (coarse gratings), afferents phase lock to the stimulus temporal frequency and thus can provide information about surface texture. These data demonstrate that fish can have the capability to sense the tactile features of their near range physical environment with fins.

KEY WORDS: Mechanosensation, Texture, Touch, Pectoral fin, Fish

INTRODUCTION

Our perception of the natural world is greatly influenced by the tactile recognition of surface features. Through touch, we gather information about the microgeometry and material properties of contacted surfaces. Texture perception and its neural encoding mechanisms have traditionally been studied in the primate hand, yet animals of all types interact with a variety of surfaces. Detail on the roughness of tree bark, the slipperiness of wet stone, or even the material composition of animal skin (i.e. fur, scales, feathers) influences perception of the physical environment and behavior. Here we explore texture sensation in a different type of vertebrate limb by investigating touch and potential texture encoding mechanisms in the pectoral fins of fishes, which are the forelimb homologs. Fish provide the opportunity to study appendage-based texture encoding in a very different context from that of previous studies as fishes are phylogenetically distant from primates, inhabit an aquatic environment, and have membranous appendages that are structurally very different from the fleshy arms, hands and digits of primate limbs.

Department of Organismal Biology and Anatomy, The University of Chicago, 1027 E. 57th Street, Chicago, IL 60637, USA.

*Author for correspondence (mhale@uchicago.edu)

A.R.H., 0000-0003-3370-7144; M.E.H., 0000-0001-5194-1220

In primates, mechanosensory skin surfaces contain an assortment of distinct afferent populations that function together to encode aspects of tactile sensation including texture. Terminating as either free nerve endings or in specialized mechanosensory cells, afferents can be broadly differentiated according to their functional response properties to sustained adaptation (i.e. slowly vs. rapidly adapting) and morphological characteristics such as receptive field size (Johnson, 2001). By integrating afferents that differentially respond to aspects of skin deformation, mechanosensory surfaces are well suited to resolving surface features that span many orders of magnitude. In the primate finger pad system, coarse textural features (on the order of millimeters) are most faithfully encoded in the spatial pattern of activation across slowly adapting type 1 (SA1) afferents that terminate in Merkel cells (Blake et al., 1997; Connor et al., 1990; Connor and Johnson, 1992; Yoshioka et al., 2001). Fine textures (on the order of micrometers), however, are encoded by texture-specific vibrations that produce characteristic temporal spike patterns in rapidly adapting (RA) afferents and Pacinian (PC) afferents, which are classified as a separate type of rapidly adapting afferent (Manfredi et al., 2014; Weber et al., 2013). SA1 and RA fibers are well suited to conveying the spatial information of contacted surfaces as a result of their small (3–5 mm) receptive field size and dense innervation in locations important for touch (Darian-Smith and Kenins, 1980; Johansson and Vallbo, 1979; Vega-Bermudez and Johnson, 1999).

Here we sought to investigate whether the fins of fish exhibit similar tactile capabilities and use the same design principles observed in touch-sensitive limbs of other vertebrate taxa. Touch has primarily been investigated in terrestrial contexts, but aquatic organisms such as fish are commonly observed to contact the bottom substrate, plants or other animals using their body and fins. Fin ray afferents have been shown to provide proprioceptive input on fin movement (Aiello et al., 2016, 2017; Williams et al., 2013) as well as sensation of pressure (Hardy et al., 2016). Nerve fibers run along the length of fin rays and terminate as either free nerve endings or expanded endings (Williams et al., 2013; Hardy et al., 2016). For some fibers, the associated sensory cells label with an antibody against cytokeratin 20, a histological marker of Merkel cells (Moll et al., 1995). As a direct link to the near-range environment, tactile feedback from fins on how contacted surfaces feel (i.e. texture) could inform a host of behaviors such as substrate associated locomotion, navigation, station holding and burying (Kasumyan, 2011). If fish touch sensation is similar to other touch-sensitive systems that exhibit spatial resolution of contacted surfaces, we would expect the receptive fields of fin ray afferents will be small (on the order of a few millimeters) and able to respond to coarse textural features of contacted surfaces.

As a model for investigating the functional capacities of touch in fins we studied the round goby (*Neogobius melanostomus*). Found on substrate types of varying roughness (Miller, 1986; Young et al., 2010), these fish rest on and interact with the bottom using their

Journal of Experimental Biology

1

large membranous pectoral fins. Pectoral fins are flexible structures, composed of bony rays held together by a membrane, which deform during motion and contact with the physical environment. Regions of the goby pectoral fin that touch the substrate were determined. We report here on the receptive field size of associated afferents, characterizing their response to coarse textures (gratings of varying spatial period) using a custom-built drum stimulator. In addition to a more nuanced understanding of pectoral fin mechanosensation and the sensory role that fins may play, particularly for substrate-associated species, this study contributes to our understanding of the evolution of appendage-based tactile sensation more broadly. By investigating texture perception in a very different context from that of primates we provide insight into the general features of touch that may occur broadly across vertebrates.

MATERIALS AND METHODS
Animals
Round Goby [*Neogobius melanostomus* (Pallas 1814)] were maintained in 40 liter aquaria at the University of Chicago (Chicago, IL, USA) under seasonal day:night light cycles with a water temperature of 15–25°C. Individuals used for physiological experiments were euthanized in a 0.5 g l^{-1} solution of MS-222 (tricaine methanesulfonate, Sigma-Aldrich) in water. All experimental procedures were carried out under University of Chicago Institutional Animal Care and Use Committee guidelines (protocol 71589 to M.E.H.).

Pectoral fin substrate contact
To assess the interaction between the pectoral fin of *N. melanostomus* and the bottom substrate during behavior, we created 3D reconstructions of the fin using a three-camera stereo setup and the R package StereoMorph (Olsen and Westneat, 2015). Fish (*n*=5) were filmed in a 21×15 cm tank under a mirror angled at 45 deg, which allowed for the simultaneous recordings of the dorsal, lateral, and anterior views. Each fish was filmed on the following three substrates: a flat piece of slate rock (20×10 cm), a 3D printed contoured bottom consisting of two mounds (5 mm high) and a vertical pane of glass to mimic how these fishes wedge themselves against the substrate. The proximal base and distal tip of each fin ray was digitized and quadratic Bézier curves were added between these points to represent the shape of each ray. Landmarks on the fin and substrate were digitized on the 2D image from each camera and then reconstructed into 3D according to the DLT calibration coefficients.

Functional properties and physiological response to textured surfaces
Electrophysiology methods followed Williams et al. (2013). Briefly, we recorded multiunit physiological responses from nerves innervating the fin rays on the medial side of the pectoral fin using glass suction electrodes. Fin rays were clamped at their proximal end and the inter-ray membrane was cut to isolate individual rays for mechanical stimuli.

We recorded the response of fin ray afferents to a proximodistal brushing stimulus in order to determine their receptive field size and firing characteristics associated with tactile motion. The tactile stimulus, performed via an actuator mounted on a voice coil positioning stage (VCS10-023-BS-01-M, H2W Technologies Inc., Valencia, CA, USA) and controlled using a programmable driver (Intelligent Servo Drive IDM640-8EI, Technosoft, Canton, MI, USA), consisted of moving a smooth rod (dimensions: 1×5 mm) perpendicularly along the length of a given fin ray. The force of fin

ray contact, measured using a scale (XP-3000; Denver Instrument Company, Arvada, CO, USA) positioned underneath the fictive fin preparation, was consistently equivalent to ~4 g throughout the duration of the stimulus. The stimulus moved 8 mm towards the distal tip of a given fin ray at 5, 10 or 20 mm s^{-1} to examine the effect of speed. Stimuli were repeated 10 times for each experiment with an inter-stimulus duration of 5 s to prevent adaptation. Multi-unit recordings were taken from the right pectoral fin of seven individuals.

To investigate whether fin ray afferents reliably encode spatial features of coarse surfaces, we recorded nerve activity in response to 3D printed gratings delivered to the medial fin ray surface using a custom-built rotating drum stimulator (Fig. 1). Gratings have been used extensively in texture-encoding experiments as their repetitive and simple spatial pattern facilitate the analysis of potential encoding mechanisms (Darian-Smith and Oke, 1980; Lederman et al., 1982; Morley and Goodwin, 1987; Yoshioka et al., 2001). The drum consisted of a series of gratings (height=1 mm, width=2 mm) created with the use of a LulzBot TAZ 6 3D printer (ABS, Aleph Objects, Loveland, CO, USA). To examine the ability of afferents to resolve surfaces of varying spatial period, the distance between elements varied between 3, 5 and 7 mm. These dimensions were chosen to mimic the grain sizes for a subset of the substrate types [i.e. coarse sand (1–2 mm grain size), granules (2–4 mm), and pebbles (4–16 mm)] that these fishes regularly encounter in their natural habitat. Round gobies are also abundant on mud (<0.06 mm grain size) as well as cobbles and boulders ranging in size from several centimeters to meters across. The drum powered by a
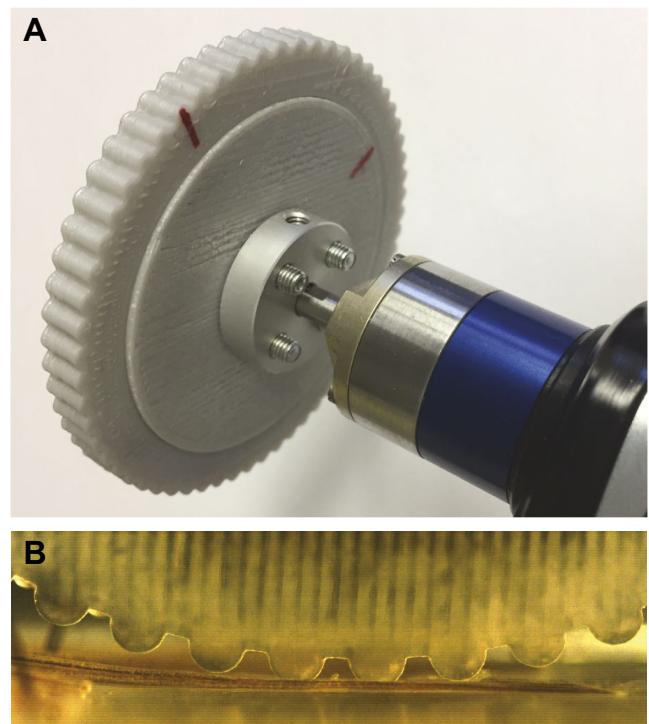
Fig. 1. Experimental setup of the rotating drum stimulator and fin preparation. (A) The rotating drum stimulator consists of 3D printed gratings (height=1 mm, width=2 mm) of varying spatial period (3, 5 or 7 mm) connected to a small DC motor that was rotated at 20, 40, 60 or 80 mm s^{-1}. (B) Each trial began with the drum positioned directly above and in light contact with a fin ray. We used still imaging and high-speed videography to ensure consistent contact across trials.

Faulhaber 2224U012SR DC motor (MicroMo Electronics, Clearwater, FL, USA) rotated at 20, 40, 60 or 80 mm s^{-1} to examine the effect of scanning speed on the afferent response. Each trial began with the drum positioned directly dorsal and in light contact with a fin ray. We used still imaging and high-speed videography to ensure consistent contact across trials. Regardless of the drum's rotational speed, gratings were presented for 3 s followed by a 5 s period of stasis and subsequent return to the original starting position before the start of the next stimulus. Five repetitions of each stimulus were presented to the fin for each speed and grating type. Video of the stimuli was recorded at 125 frames s^{-1} using a Fastcam APX RS camera (Photron, San Diego, CA) and synchronized with the electrical recordings using an external signal.

Physiological data analysis

Data were sampled at 100 kHz, down-sampled to 10 kHz, and analyzed in MATLAB 2017a (Mathworks, Natick, MA, USA). To identify and sort individual units from our extracellular recordings, we used a modified version of the spike sorting algorithm, Wave_clus (Quiroga et al., 2004). Wave_clus provides a semi-automatic method of spike sorting based on wavelet decomposition and superparamagnetic clustering (SPC). To detect spikes, we set a 2.5 ms absolute refractory period and used an amplitude threshold 5-times the standard deviation of the background noise. Statistical analyses of the mechanical stimulation data were performed using JMP software (SAS, Cary, NC, USA). We used linear mixed-effect models that consider repeated measures to evaluate our fixed effects (i.e. stimulus speed, grating spatial period) on a variety of response variables. For all such models, we used subject ID as a random factor.

We applied a set of criteria to define the first and last action potential associated with each afferent's receptive field in response to a proximodistal brushing stimuli. First, action potentials within 50 ms after onset of the stimulus were excluded from subsequent analyses to eliminate transient effects associated with the initial movement of the rod across the fin at stimulus onset. Spikes occurred during this 50 ms period in 63 of the 240 stimulus presentations analyzed and typically consisted of just a single action potential. In an effort to exclude non-stimulus evoked activity, we applied a firing rate threshold (mean+s.d.) based on the ISI of spikes occurring during a 1 s pre-stimulus baseline period. However, as pre-stimulus activity was typically absent we applied an additional firing rate threshold (mean+5*s.d.) based on the ISI of spikes that occurred during the stimulus. Given the stimulus speed (5, 10 or 20 mm s^{-1}) and the duration between the first and last action potential that satisfied these conditions, we calculated the linear size of each afferent's receptive field.

For afferents that exhibited activity to the sustained indentation of the probe after stimulus offset, we determined the dynamic and static phase of the exhibited slowly adapting response. We defined the dynamic phase of the adaption as the time between stimulus offset and the data point in which the moving s.d. (window length=3) of the instantaneous firing rate for two consecutive spikes were both below one. The static phase continued immediately from this plateau in the firing rate for two additional seconds. The coefficient of variation (CV), a measure of spike regularity, for each stimulus in the static phase was calculated as the standard deviation of static phase ISIs divided by the mean static ISI.

To calculate the degree to which an afferent's response to textured surfaces matched or was tuned to the stimulus frequency we calculated the vector strength of the response (Goldberg and Brown, 1969). Vector strength, a measure of phase locking between a periodic stimulus and a response, ranges from 0 for uniform firing

across all phases of the stimulus to 1 for perfectly synchronized firing at only one phase of the stimulus. We calculated the vector strength of the response for each trial (n=5 for each combination of scanning speed and spatial period). Vector strength was calculated from all spikes across 2 s of steady-state spiking data that began 0.5 s after stimulus onset and ended 0.5 s before stimulus offset. We also compared the mean experimental vector strength value to that expected from firing unrelated to the periodicity of the stimulus. The mean firing rate (spikes s^{-1}) of each experimental trial was used to generate 200 Poisson spike trains. We calculated the vector strength of these simulated spike trains and then randomly and with replacement selected one value from each trial (n=5 for each for each combination of scanning speed and spatial period) to generate a mean simulated vector strength value. This process was repeated 10,000 times in order to get the distribution of vector strengths arising from the null hypothesis that there is no phase locking to the grating period.

RESULTS

Pectoral fin substrate contact

Analysis shows that the pectoral fins of *N. melanostomus* regularly contact the bottom substrate while the fish is at rest (Fig. 2). The pectoral fin rays exhibit multiple branches distally that together with expansive inter-ray membranes readily conform to the contours of the bottom substrate. While the number and identity of fin rays in contact with the substrate varied across trials conducted on the three substrate types, we observed that substrate contact along the span of the fin is substantial. During these behavioral trials we observed that all but the dorsalmost (i.e. leading edge) fin rays touched the bottom. Along the proximodistal axis, contact was found to be localized to the distal half of a given ray. Similarly to other limbs, the functional demands for tactile feedback are not uniform across the fin and we subsequently targeted fin regions identified to regularly contact surfaces during our physiological experiments.

Receptive field properties

We determined receptive field size and firing characteristics of fin ray afferents with a proximodistal brushing stimulus applied to the fin. For all physiological experiments conducted in this study, we targeted the ventral surface of the distal half of fin rays, previously identified as regularly contacting the substrate during routine behavior (Fig. 2). The probe moved 8 mm along a given fin ray at 5, 10 or 20 mm s^{-1}. From our multi-unit recordings, we identified afferents (n=8) whose activity occurred completely within the stimulus area allowing for the determination of receptive field length. Afferents whose activity was cut off by either the start or stop of the stimulus were excluded from the analysis as the true distance with which the afferent could have responded was unknown. Trials at a given speed were repeated 10 times to control for possible variability in the application of the stimulus as well as to investigate the consistency of the afferent response. We found that the spatiotemporal discharge patterns were visually similar across trials, highlighting the consistency with which fin ray afferents respond to repeated tactile stimuli (Fig. 3A).

Fin ray afferents exhibited small receptive fields, similar in size to those of the SA1 and RA afferents observed in primates. We found that the mean receptive field diameter of recorded afferents was 2.28–5.07 mm (Fig. 3B). In addition, we asked whether these afferents exhibit response characteristics to tactile motion that are similar to those of mammals. As the scanning speed increased and the duration of the stimulus decreased, we predictably found a significant decrease in the duration of stimulus evoked activity ($F_{2,14}$=74.61, P<0.0001) and the number of evoked spikes
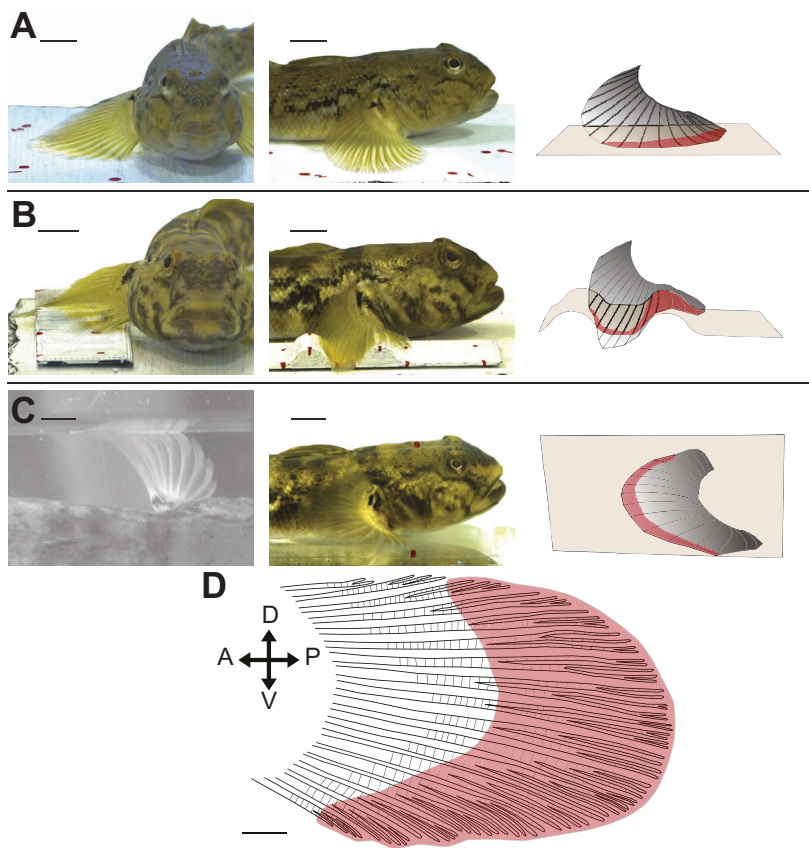
Fig. 2. Physical interaction between the pectoral fin of stationary *Neogobius melanostomus* and the bottom substrate on three substrate types. (A) Anterior (left) and lateral (middle) camera views of a round goby resting on a flat piece of slate rock (20×10 cm). Lateral view of a 3D model (right) illustrating the position of the pectoral fin (gray) including each of the 19 fin rays relative to the bottom substrate (tan colored trapezoid). Regions of the pectoral fin observed to touch the bottom are shaded red. Fin ray contact on a flat surface is localized towards the distal tips of trailing edge fin rays. (B) Anterior (left) and lateral (middle) camera views of a pectoral fin resting on a 3D printed bottom consisting of two mounds (5 mm high). Camera images and lateral view of 3D model (right) show that the fin is flexible and readily molds to the shape of the bottom substrate. Fin ray contact (red) is more substantial across the fin surface. (C) Posterior (left) and lateral (middle) camera views of a pectoral fin propped against a vertically oriented pane of glass to mimic how these fishes often wedge themselves against and between objects. Scale bars: 1 cm. (D) Illustration showing regions of the pectoral fin marked in red that likely contact surfaces during routine behavior. Shading is based on experimental and observation data in aquaria and does not reflect the presence or absence of any underlying sensory morphology. Scale bar: 2 mm.

($F_{2,14}$=64.56, P<0.0001) (Fig. 4A,B). Mechanoreceptor firing rates in mammalian systems have been shown to increase as the speed of objects scanned across the skin increases (Essick and Edin, 1995; Goodwin and Morley, 1987; Greenspan, 1992). Similarly, we found that the firing rate of these fin afferents significantly increased as the scanning speed of the probe increased from 5 to 20 mm s^{-1} ($F_{1,7}$=7.34, P=0.0302) (Fig. 4C). The velocity-dependent responsiveness of these afferents may reflect the faster progression and/or greater intensity of the different phases (i.e. skin compression, stretch, indentation) of the tactile stimulus as the probe moves across the fin surface at increased scanning speeds.

We also recorded from four additional afferents (*n*=4 afferents from three fish; 120 total stimulus presentations) that continued to fire well after the stimulus stopped moving, indicative of a slowly adapting response to the sustained indentation of the probe. The response, characterized by a sharp decrease in firing rate shortly after stimulus offset followed by an extended duration of tonic firing, is similar to that seen in SA1 units in other systems (Fig. S1). When averaged across trials, the spike rate (spikes s^{-1}) during the period of prolonged indentation was 13.63±3.71 (mean±s.d.). We calculated the coefficient of variation (CV) of the interspike intervals to determine the regularity of their static-phase firing rates. We found that these fin ray afferents displayed mean CVs ranging from 0.35–0.58 suggestive of high ISI variability and further support of the functional similarity between the slowly adapting afferents of fish and those observed in mammalian taxa (Iggo and Muir, 1969; Knibeştöl, 1975; Wellnitz et al., 2010).

Texture encoding

Targeting regions of the fin that routinely contact the bottom, we identified fin ray afferents that exhibit a phase-locked response to the periodic structure of coarse gratings. Complete data sets consisting of the response to three sets of gratings (spatial periods of 3, 5 or 7 mm) moving at four different speeds (20, 40, 60, 80 mm s^{-1}) were recorded from an additional six neurons. Given the spatial periods and the scanning speeds employed, the stimulus temporal frequency (scanning speed/grating spatial period) ranged from ~3 Hz to 27 Hz.

Afferents were responsive to individual gratings as they moved across their receptive field (Fig. 5). In order to measure the strength of entrainment to the periodic structure of the coarse gratings, we computed the vector strength of the afferent response. A vector strength of zero corresponds to uniform firing across all phases of the grating cycle whereas a value of one corresponds to firing at only one phase location relative to each passing grating. We found that afferents exhibited high vector strength values, consistently above 0.4, regardless of the grating spatial period or its corresponding temporal frequency (Fig. 6). Furthermore, mean vector strength values for each combination of spatial period and scanning speed were significantly higher than expected by chance (*P*<0.001; Fig. S2). The spatial period of the grating had a significant effect on the strength of the entrainment ($F_{2,10}$=5.4792, *P*<0.0247). For example, as the grating spatial period increased from 3 to 7 mm, the mean vector strength of the response when pooled across scanning speeds significantly increased from 0.54 to 0.73 (Tukey-HSD, *P*=0.0197). Changes to scanning speed however, did not have a significant effect on the magnitude of entrainment in response to gratings with a given spatial period of 3 mm ($F_{3,15}$=0.9157, *P*=0.45), 5 mm ($F_{3,15}$=0.5542, *P*=0.65) or 7 mm ($F_{3,15}$=2.0402, *P*=0.15), suggesting that the phase locking is robust across a wide spectrum of biologically relevant scanning speeds.

Gratings are well defined if any two of the following stimulus parameters are known: spatial period, scanning speed and temporal
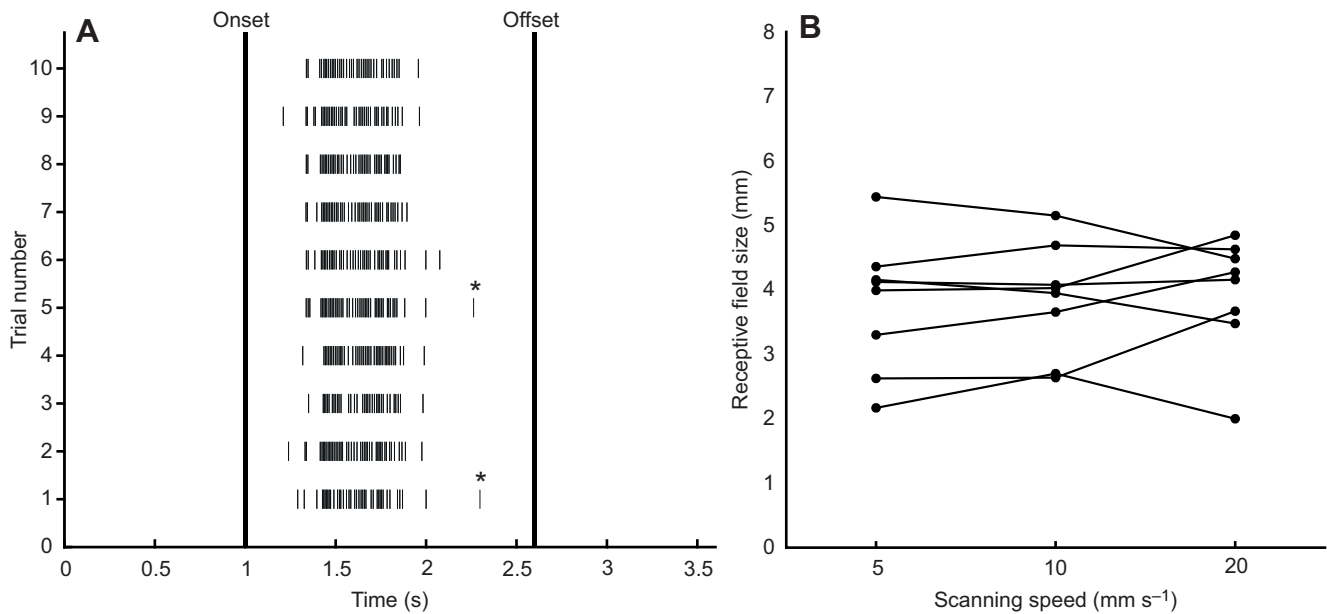
Fig. 3. Determination of fin ray afferent receptive field size to tactile motion. (A) Spike raster of a representative afferent showing the response to a proximodistal brushing stimulus moving across 8 mm at 5 mm s^{-1}. Spikes marked with an asterisk were excluded from analyses based on a firing rate threshold (see Materials and Methods). (B) Fin ray afferents have small receptive fields, similar in size to those of the SA1 and RA afferents observed in primates. Given the stimulus speed (5, 10 or 20 mm s^{-1}) and the duration between the first and last action potential for each trial, we calculated the linear extent of each afferent's receptive field. The mean receptive field size of afferents ranged from 2.28 to 5.07 mm. Each point represents the mean of 10 trials and points connected by a line belong to the same afferent (n=8 afferents). Mean and standard deviation values are reported in Table S1.

frequency. As the phase-locked response provides reliable information regarding the temporal frequency, we investigated whether mean firing rate or the mean number of spikes elicited per grating ridge faithfully encode either the scanning speed or spatial period. When the spatial period was held constant, we found that changes to scanning speed, and thus the stimulus temporal frequency, had a significant effect on the normalized mean afferent firing rate (spikes s^{-1}) for gratings with a 3 mm ($F_{3,15}$=7.4793, P=0.0027), 5 mm ($F_{3,15}$=4.8636, P=0.0147) and 7 mm ($F_{3,15}$=4.2052, P=0.0240) spatial period (Fig. 7A). While we observed a significant increase in

the mean firing rate with changes in scanning speed from 20 to 80 mm s^{-1} for each grating, the response was invariant to scanning speeds above 40 mm s^{-1}. Likewise, we did not observe a significant effect of changes to spatial period when the scanning speed was held constant at 20 ($F_{2,10}$=0.4563, P=0.6462), 40 ($F_{2,10}$=0.1300, P=0.8795), 60 ($F_{2,10}$=3.338, P=0.0775) or 80 mm s^{-1} ($F_{2,10}$=0.8523, P=0.4552) (Fig. 7B).

We determined the average number of spikes produced per contact with a grating by dividing the afferent firing rate by the stimulus temporal frequency. In response to frequencies above
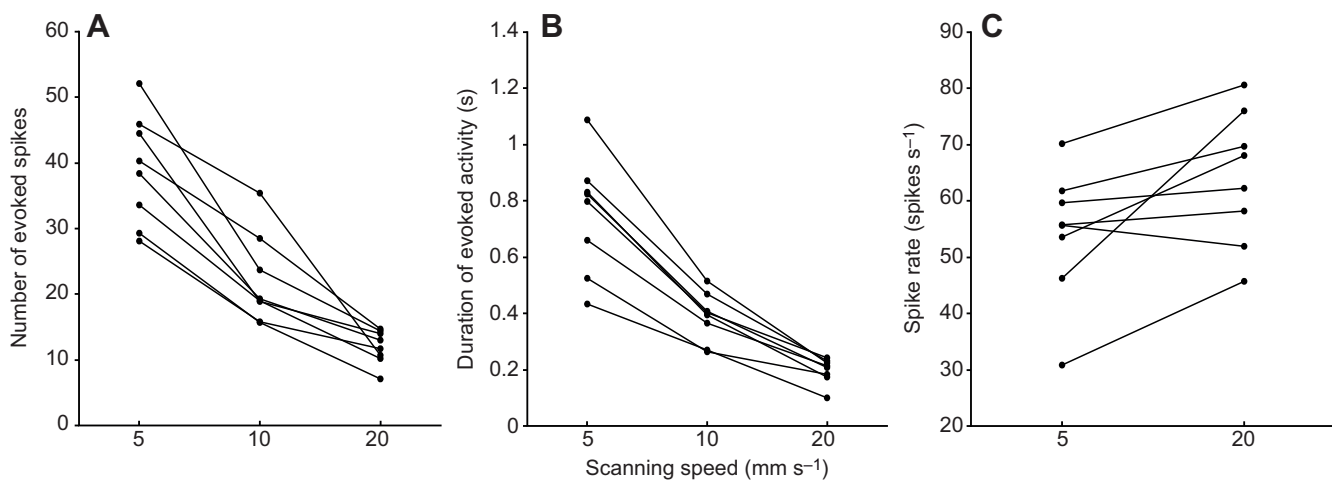
Fig. 4. Afferent response to a proximodistal brushing stimuli. (A) Mean number of stimulus-evoked spikes versus scanning speed. (B) Mean duration of stimulus-evoked activity versus scanning speed. The number of evoked spikes ($F_{2,14}$=64.56, P<0.0001) and the duration of stimulus evoked activity ($F_{2,14}$=74.61, P<0.0001) significantly decreased with increasing stimulus speeds as the probe spent less time in contact with the fin ray surface. (C) Mean firing rate versus scanning speed. Similar to mammalian mechanoreceptors, the firing rate of fin afferents significantly increased as the scanning speed of the probe increased from 5 to 20 mm s^{-1} ($F_{1,7}$=7.34, P=0.0302). As the speed of the probe increased, the faster rate of change in stimulus components (i.e. compression, stretch, indentation) are reflected in the higher discharge rates. Each point represents the mean of 10 trials and points connected by a line belong to the same afferent (n=8 afferents). Mean and standard deviation values reported in Table S1.
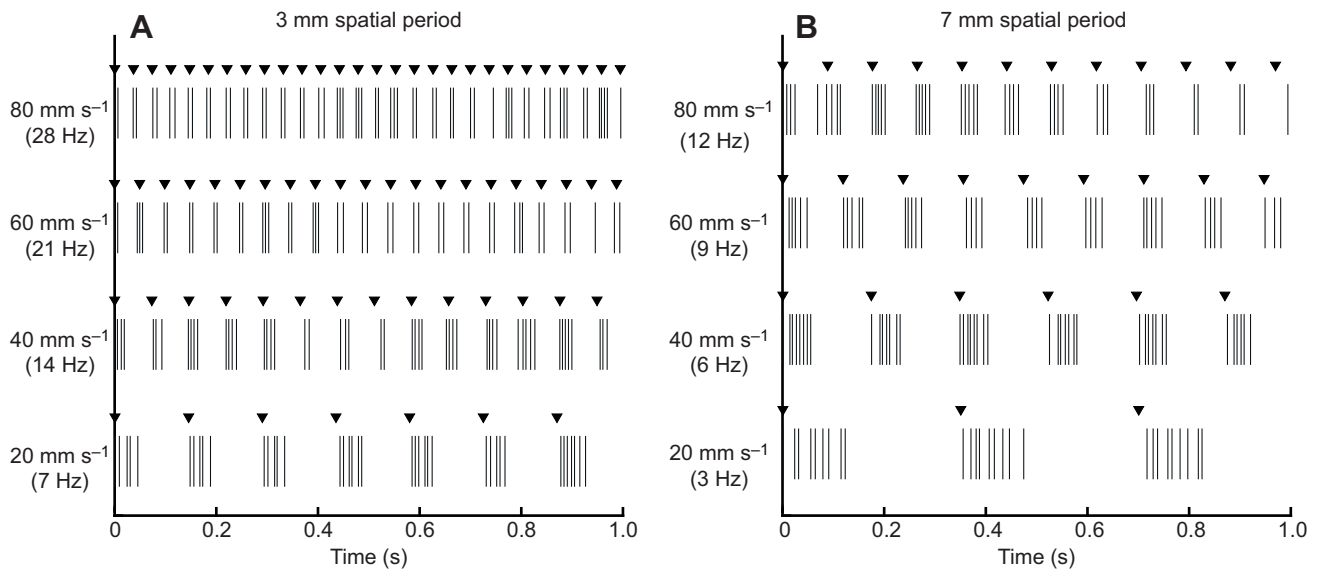
Fig. 5. Afferent spiking in response to coarse gratings. Each grouping of raster plots shows the representative response of a fin ray afferent to gratings with a 3 mm (A) or 7 mm (B) spatial period moving over its receptive field. The scanning speed (20, 40, 60 and 80 mm s^{-1}) as well as the corresponding stimulus temporal frequency are indicated to the left of each raster. Arrowheads mark the time separation between successive gratings. The first arrowhead in each plot has been aligned to the first spike associated with a grating discharge. We found that afferents (n=6) were responsive to each successive grating and that the average number of spikes elicited by each grating significantly decreased as the scanning speed increased from 20 to 80 mm s^{-1} (Tukey-HSD, $P \leq 0.0001$).

10 Hz, afferents fired 1–3 times per contact with a grating. Occasionally, the mean interspike interval closely matched that of the stimulus temporal period (1/temporal frequency) indicating that the afferent fired exactly once as each grating passed over its receptive field. At the lowest frequency we tested however (∼3 Hz for 7 mm spatial period gratings moving at 20 mm s^{-1}), the average spike count was 8.82±3.39 (mean±s.d.). When the spatial period was held constant, we found that the average number of spikes elicited per contact with a grating significantly decreased as the scanning speed increased from 20 to 80 mm s^{-1} for each of the three sets of gratings (Tukey-HSD, $P \leq 0.0001$) (Fig. 7C). When the scanning speed was held constant however, we found that

only at the lowest scanning speeds of 20 mm s^{-1} was spike number significantly different for each spatial period (Fig. 7D). Taken together, mean firing rate and spike number do not faithfully encode either the grating spatial period or scanning speed across the experimental range of stimuli tested here.

DISCUSSION
From these results we conclude that: (1) pectoral fins can have the capability to respond to the coarse features of textured surfaces and tactile motion, and (2) the morphology and response properties to touch reported here for the pectoral fin of a bottom-dwelling fish are consistent with those of mammalian systems studied previously.
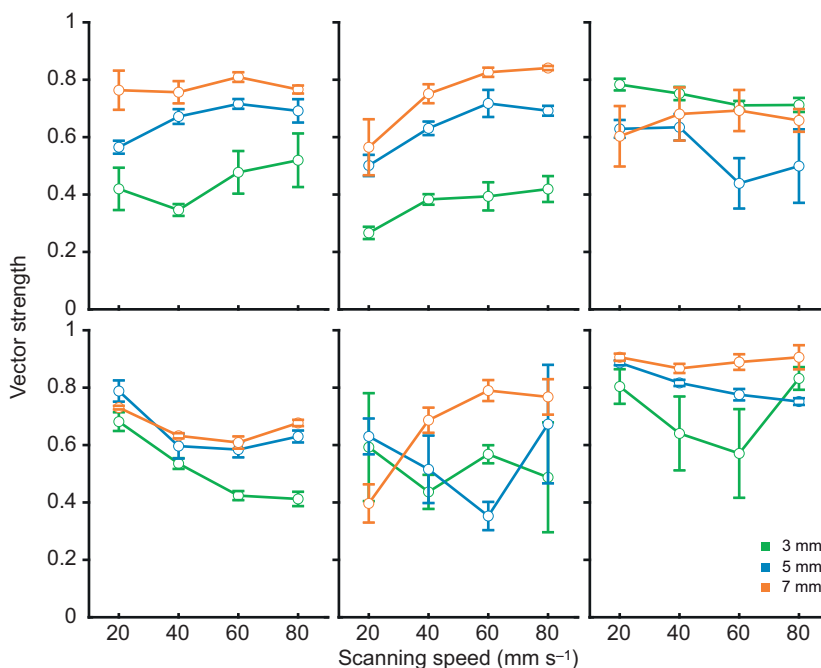
Fig. 6. The strength of entrainment (i.e. phase locking) to the spatial period of coarse gratings. Vector strength, a measure of phase locking between a periodic stimulus and a neural response, ranges from 0 for uniform firing across all phases of the stimulus to 1 for perfectly synchronized firing at only one phase location relative to each passing stimulus. Each plot shows the response from an individual afferent (n=6) to gratings with a 3 mm (green), 5 mm (blue), and 7 mm (orange) scanned across the fin at 20, 40, 60, and 80 mm s^{-1}. Data points are the mean (n=5 trials) vector strength value at a given combination of grating spatial period and scanning speed. Afferents exhibited high vector strength values, consistently above 0.4, regardless of the grating spatial period or its corresponding temporal frequency. Mean vector strength values for each combination of spatial period and scanning speed were significantly higher than expected by chance ($P<0.001$). The high degree of phase locking provides precise information on the temporal frequency on coarse gratings independent of the grating spatial period or scanning speed. Error bars represent one standard deviation.

The paired fins of fishes serve in diverse behaviors such as locomotion, posture, respiration, feeding and brooding (Gibb et al., 1994; Gosline, 1994; Green et al., 2011; Higham, 2007; Künzler and Bakker, 2000; Taft et al., 2008; Westneat, 1996). Previous studies on the filamentous pelvic rays of hake (*Urophycis chuss*) (Bardach and Case, 1965) as well as the membranous pectoral fins of bluegill sunfish (*Lepomis macrochirus*) (Williams et al., 2013) and wrasse (Family Labridae) (Aiello et al., 2017) have shown that fin ray afferents provide proprioceptive feedback in response to movement and deflection of the rays. Hardy et al. (2016) reported that afferents innervating the pectoral fin of pictus catfish (*Pimelodus pictus*), a bottom-dwelling species, respond to pressure and light surface brushing, thus expanding the known sensory repertoire of paired appendages in fishes to include touch. Given the sensitivity to touch shown in fins, we sought to investigate whether fins exhibit similar tactile capabilities and characteristics observed in touch-sensitive limbs of other vertebrate taxa.

Fish frequently contact the bottom substrate, plants or other animals using their fins. Observations of the round goby on a variety of substrate types indicate that a significant portion of the pectoral fin contacts and molds to the contours of the bottom while at rest (Fig. 1). Beyond the simple sensation of contact, fin ray feedback on how contacted surfaces feel (i.e. roughness, slipperiness, etc.) could be important for habitat selection as well as in a variety of other behaviors such as substrate-associated locomotion, navigation, posture and burying. When selecting suitable habitat, for example, bottom-associated fish often exhibit clear preferences for particular types of substrate such as silt, sand or pebbles (Gibson and Robb, 2000; Moles and Norcross, 1995). Compared with the terrestrial environment, the aquatic realm imposes unique sensory challenges as the amount of visible light available for animals to utilize rapidly decreases with depth and is negatively affected by the turbidity of water. While fish can utilize their visual and lateral line systems to discern physical features of their immediate surroundings, sensitivity to differences in the material and geometric
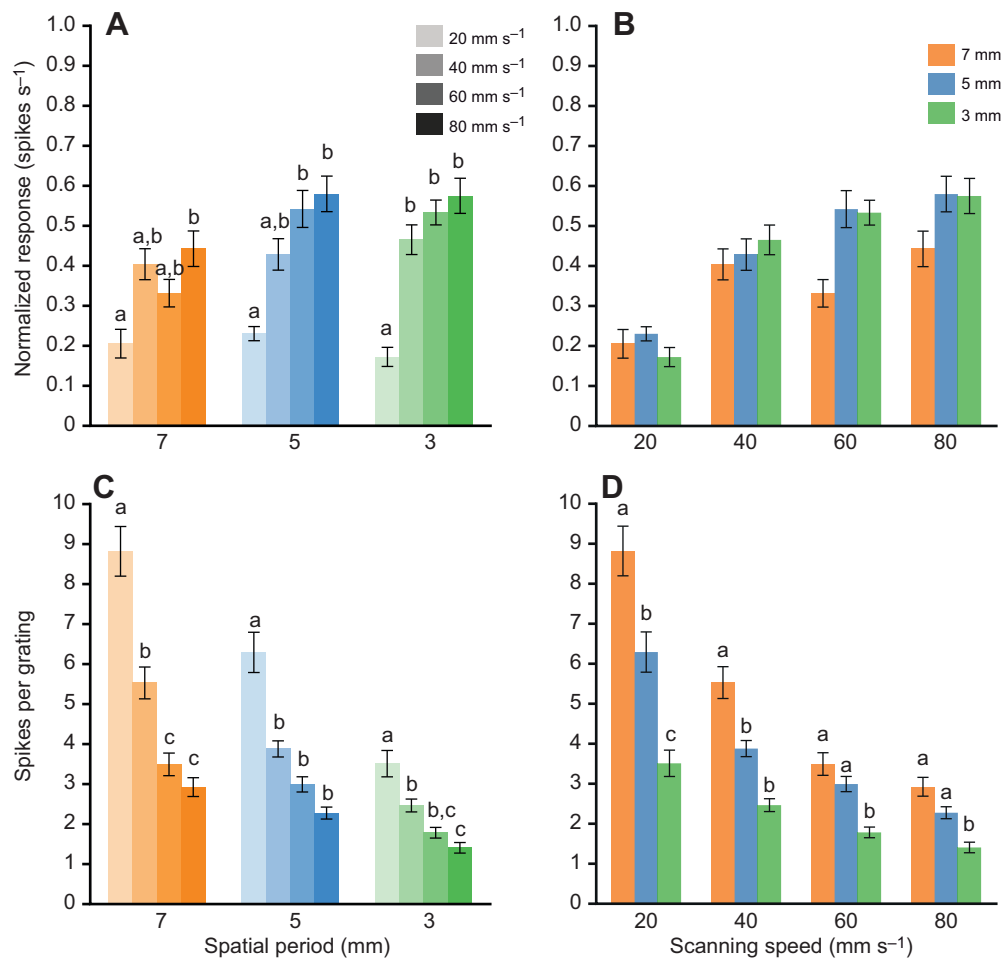
Fig. 7. Measures of the mean afferent response when either spatial period or scanning speed is held constant. (A) When the spatial period was held constant, changes to scanning speed and thus the stimulus temporal frequency, had a significant effect on the normalized mean afferent firing rate (spikes s^{-1}) for gratings with a 3 mm ($F_{3,15}$=7.4793, P=0.0027), 5 mm ($F_{3,15}$=4.8636, P=0.0147) and 7 mm ($F_{3,15}$=4.2052, P=0.0240) spatial period. While afferents responded with a significant increase in the mean firing rate with changes in scanning speed from 20 to 80 mm s^{-1} for each grating, the response was invariant to scanning speeds above 20 mm s^{-1}. (B) The spatial period of the grating did not have a significant effect on the response when the scanning speed was held constant at 20 ($F_{2,10}$=0.4563, P=0.6462), 40 ($F_{2,10}$=0.1300, P=0.8795), 60 ($F_{2,10}$=3.338, P=0.0775) or 80 mm s^{-1} ($F_{2,10}$=0.8523, P=0.4552). (C) The average number of spikes elicited per contact with a grating significantly decreased as the scanning speed increased from 20 to 80 mm s^{-1} for each of the three sets of gratings (Tukey-HSD, P≤0.0001). Key as shown in A. (D) When the scanning speed was held constant however, only at the lowest scanning speeds of 20 mm s^{-1} was spike number significantly different for each grating. Key as shown in B. Error bars denote the s.e.m. across gratings and scanning speeds. Significant differences between groups are indicated with different letters.

characteristics of contacted surfaces provides direct feedback on mechanical characteristics of surfaces and presumably take on a more consequential role in low-visibility conditions where other sensory modalities may not be effective.

Physiological analysis of the pectoral fin ray afferent response demonstrates that fins are well suited to encoding coarse textural features of contacted surfaces. We found that a subset of afferents exhibited receptive fields that span 2–5 mm in length. The presence of small receptive fields within fins suggest their utility for sensing mechanical events with a high degree of spatial resolution. Using a rotating drum stimulator, we found that afferents respond to coarse gratings when scanned across their receptive fields with a phase-locked response to the temporal frequency of the stimulus. The degree of phase locking as measured by vector strength was significantly higher than expected by chance for all gratings tested and found to be invariant to changes in scanning speed. Changes in scanning speed while the spatial period of the grating was held constant had predictable effects on the afferent response and showed similarities to the SA response observed by Morley and Goodwin (1987) in the monkey finger pad. Occasionally at high scanning speeds, we observed that the mean interspike interval closely matched that of the stimulus temporal period. This precise match between interspike interval and temporal period in response to coarse gratings has been reported by Darian-Smith and Oke (1980) for SA1, Pacinian and RA fibers in the monkey finger pad. While these authors reported that multiple discharges per grating were uncommon, Morley and Goodwin (1987), as well as the data presented here, show that afferents typically responded to each grating with multiple spikes. This discrepancy between studies could be due to differences in contact force, range of temporal frequencies examined, or grating dimensions.

In this work we present the first investigation of fin ray sensation of texture, utilizing coarse gratings to facilitate matching stimulus features to the afferent response. When scanned across the skin, the temporal frequency of gratings is dependent on both spatial period and scanning speed. It is therefore possible for gratings with different spatial periods to generate identical temporal periods simply by modulating the scanning speed. Given this fact and lack of a response feature (i.e. firing rate, spike number per grating) that alone faithfully encodes either the spatial period or scanning speed across the experimental range of stimuli tested, individual fin ray afferents may not unequivocally encode the spatial structure of gratings. While phase-locked responses of individual afferents provide precise information on the temporal frequency, spatial information about contacted surface features likely depends on information signaled across the afferent population. In primates, the spatial structure of coarse surfaces is best encoded in the spatial variation of slowly adapting type 1 (SA1) afferent firing rates (Blake et al., 1997; Connor et al., 1990; Connor and Johnson, 1992; Weber et al., 2013; Yoshioka et al., 2001). Calculated as the difference in mean firing rates between fibers with receptive field centers separated by a fixed distance, spatial variation on a scale of ∼2 mm was found to most closely correlate with ratings of perceived roughness (Connor et al., 1990). Given the high innervation density of the primate hand, this distance corresponds to firing rate differences between adjacent or nearly adjacent receptors (Darian-Smith and Kenins, 1980; Johansson and Vallbo, 1979).

The finding that fin ray afferents have small receptive fields and that their responses are modulated by the periodic structure of coarse gratings provides support for the hypothesis that fish utilize a spatial encoding mechanism for coarse textures similar to that discussed above for primates. To test this hypothesis, it will be necessary to determine the position and density of mechanoreceptors within fins. Touch-sensitive membranes of other animals often exhibit localized regions of high sensory ending density that facilitate greater sensitivity and an increased spatial resolution of tactile stimuli (Gentle and Breward, 1986; Gottschaldt and Lausmann, 1974; Johansson and Vallbo, 1979; Sawyer and Catania, 2016). It is unknown whether fins exhibit the necessary innervation density, particularly in regions of the fin known to contact surfaces, to utilize a spatial mechanism for texture coding. In addition to estimates of mechanoreceptor density, the construction of spatial event plots would facilitate a more in-depth look at how features of contacted surfaces are spatially represented across the receptive field. For coarse textures such as gratings and embossed dot patterns scanned across the monkey finger pad, scanning event plots show that the spatial structure of the stimulus is well preserved in the spatial pattern of activation in SA1 and, to a lesser extent, RA afferents (Connor and Johnson, 1992; Phillips et al., 1992; Weber et al., 2013). Knowledge on mechanoreceptor density and the spatial resolution of fin ray afferents would better facilitate comparisons with known texture-encoding mechanisms.

These data demonstrate that the pectoral fins in the round goby, and we postulate fins in general, can gather information about the coarse structure of contacted surfaces. Fins had traditionally been thought of as primarily motor devices, but a growing body of literature has shown that fins function as sensors capable of providing precise feedback on fin ray position and movement, as well as touch-related events. Given previous studies across an ecologically diverse group of fishes showing the ability to encode information about the static and dynamic aspects of mechanosensory stimuli, we hypothesize that this sensitivity to contacted surface features is widespread among fishes. The sensitivity to and resolution of tactile stimuli presumably varies amongst species and among fins as the ecology of each species will influence the functional demands for touch. To understand the spatial resolution of the fin ray sensory system to contacted surfaces, future investigations would benefit from employing fine gratings (i.e. spatial periods closer to 1 mm), embossed dot patterns or more naturalistic textures that span the range of textures found in the natural environment. The findings presented here of primate hand-like touch in the fins of a fish also suggests that the appendage-based sensory apparatus needed for the tactile exploration of the physical environment arose in vertebrate limbs before the evolution of sarcopterygians.

Author contributions
Conceptualization: A.R.H., M.E.H.; Methodology: A.R.H., M.E.H.; Software: A.R.H.; Validation: A.R.H.; Formal analysis: A.R.H., M.E.H.; Investigation: A.R.H.; Resources: A.R.H., M.E.H.; Data curation: A.R.H.; Writing - original draft: A.R.H.; Writing - review & editing: A.R.H., M.E.H.; Visualization: A.R.H., M.E.H.; Supervision: M.E.H.; Project administration: M.E.H.; Funding acquisition: A.R.H., M.E.H.

Data availability
Data are available from Dryad (Hardy and Hale, 2020): h9w0vt4gb

Supplementary information
Supplementary information available online at
https://jeb.biologists.org/lookup/doi/10.1242/jeb.227280.supplemental

References

Aiello, B. R., Stewart, T. A. and Hale, M. E. (2016). Mechanosensation in an adipose fin. *Proc. R. Soc. B* **283**, 20152794. doi:10.1098/rspb.2015.2794

Aiello, B. R., Westneat, M. W. and Hale, M. E. (2017). Mechanosensation is evolutionarily tuned to locomotor mechanics. *Proc. Natl. Acad. Sci. USA* **114**, 4459-4464. doi:10.1073/pnas.1616839114

Bardach, J. E. and Case, J. (1965). Sensory capabilities of the modified fins of squirrel hake (*Urophycis chuss*) and searobins (*Prionotus carolinus* and *P. evolans*). *Copeia* **1965**, 194-206. doi:10.2307/1440724

Blake, D. T., Hsiao, S. S. and Johnson, K. O. (1997). Neural coding mechanisms in tactile pattern recognition: the relative contributions of slowly and rapidly adapting mechanoreceptors to perceived roughness. *J. Neurosci.* **17**, 7480-7489. doi:10.1523/JNEUROSCI.17-19-07480.1997

Connor, C. E. and Johnson, K. O. (1992). Neural coding of tactile texture: comparison of spatial and temporal mechanisms for roughness perception. *J. Neurosci.* **12**, 3414-3426. doi:10.1523/JNEUROSCI.12-09-03414.1992

Connor, C. E., Hsiao, S. S., Phillips, J. R. and Johnson, K. O. (1990). Tactile roughness: neural codes that account for psychophysical magnitude estimates. *J. Neurosci.* **10**, 3823-3836. doi:10.1523/JNEUROSCI.10-12-03823.1990

Darian-Smith, I. and Kenins, P. (1980). Innervation density of mechanoreceptive fibres supplying glabrous skin of the monkey's index finger. *J. Physiol.* **309**, 147-155. doi:10.1113/jphysiol.1980.sp013500

Darian-Smith, I. and Oke, L. E. (1980). Peripheral neural representation of the spatial frequency of a grating moving across the monkey's finger pad. *J. Physiol.* **309**, 117-133. doi:10.1113/jphysiol.1980.sp013498

Essick, G. K. and Edin, B. B. (1995). Receptor encoding of moving tactile stimuli in humans. II. The mean response of individual low-threshold mechanoreceptors to motion across the receptive field. *J. Neurosci.* **15**, 848-864. doi:10.1523/jneurosci.15-01-00848.1995

Gentle, M. J. and Breward, J. (1986). The bill tip organ of the chicken (*Gallus gallus var. domesticus*). *J. Anat.* **145**, 79-85.

Gibb, A., Jayne, B. and Lauder, G. (1994). Kinematics of pectoral fin locomotion in the bluegill sunfish *Lepomis macrochirus*. *J. Exp. Biol.* **189**, 133-161.

Gibson, R. and Robb, L. (2000). Sediment selection in juvenile plaice and its behavioural basis. *J. Fish Biol.* **56**, 1258-1275. doi:10.1111/j.1095-8649.2000.tb02138.x

Goldberg, J. M. and Brown, P. B. (1969). Response of binaural neurons of dog superior olivary complex to dichotic tonal stimuli: some physiological mechanisms of sound localization. *J. Neurophysiol.* **32**, 613-636. doi:10.1152/jn.1969.32.4.613

Goodwin, A. W. and Morley, J. W. (1987). Sinusoidal movement of a grating across the monkey's fingerpad: representation of grating and movement features in afferent fiber responses. *J. Neurosci.* **7**, 2168-2180. doi:10.1523/JNEUROSCI.07-07-02168.1987

Gosline, W. A. (1994). Function and structure in the paired fins of scorpaeniform fishes. *Environ. Biol. Fishes* **40**, 219-226. doi:10.1007/BF00002508

Gottschaldt, K.-M. and Lausmann, S. (1974). The peripheral morphological basis of tactile sensibility in the beak of geese. *Cell Tissue Res.* **153**, 477-496. doi:10.1007/bf00231542

Green, M. H., Ho, R. K. and Hale, M. E. (2011). Movement and function of the pectoral fins of the larval zebrafish (*Danio rerio*) during slow swimming. *J. Exp. Biol.* **214**, 3111-3123. doi:10.1242/jeb.057497

Greenspan, J. D. (1992). Influence of velocity and direction of surface-parallel cutaneous stimuli on responses of mechanoreceptors in feline hairy skin. *J. Neurophysiol.* **68**, 876-889. doi:10.1152/jn.1992.68.3.876

Hardy, A. and Hale, M. (2020). Data from: Sensing the structural characteristics of surfaces: texture encoding by a bottom-dwelling fish, v3. *Dryad Dataset*. doi:10.5061/dryad.h9w0vt4gb

Hardy, A. R., Steinworth, B. M. and Hale, M. E. (2016). Touch sensation by pectoral fins of the catfish *Pimelodus pictus*. *Proc. R. Soc. Lond. B Biol. Sci.* **283**, 20152652. doi:10.1098/rspb.2015.2652

Higham, T. E. (2007). Feeding, fins and braking maneuvers: locomotion during prey capture in centrarchid fishes. *J. Exp. Biol.* **210**, 107-117. doi:10.1242/jeb.02634

Iggo, A. and Muir, A. R. (1969). The structure and function of a slowly adapting touch corpuscle in hairy skin. *J. Physiol.* **200**, 763-796. doi:10.1113/jphysiol.1969.sp008721

Johansson, R. S. and Vallbo, A. B. (1979). Tactile sensibility in the human hand: relative and absolute densities of four types of mechanoreceptive units in glabrous skin. *J. Physiol.* **286**, 283-300. doi:10.1113/jphysiol.1979.sp012619

Johnson, K. O. (2001). The roles and functions of cutaneous mechanoreceptors. *Curr. Opin. Neurobiol.* **11**, 455-461. doi:10.1016/S0959-4388(00)00234-8

Kasumyan, A. O. (2011). Tactile reception and behavior of fish. *J. Ichthyol.* **51**, 1035-1103. doi:10.1134/S003294521111004X

Knibestöl, M. (1975). Stimulus-response functions of slowly adapting mechanoreceptors in the human glabrous skin area. *J. Physiol.* **245**, 63-80. doi:10.1113/jphysiol.1975.sp010835

Künzler, R. and Bakker, T. C. M. (2000). Pectoral fins and paternal quality in sticklebacks. *Proc. R. Soc. Lond. B Biol. Sci.* **267**, 999-1004. doi:10.1098/rspb.2000.1102

Lederman, S. J., Loomis, J. M. and Williams, D. A. (1982). The role of vibration in the tactual perception of roughness. *Percept. Psychophys.* **32**, 109-116. doi:10.3758/BF03204270

Manfredi, L. R., Saal, H. P., Brown, K. J., Zielinski, M. C., Dammann, J. F., , III, Polashock, V. S. and Bensmaia, S. J. (2014). Natural scenes in tactile texture. *J. Neurophysiol.* **111**, 1792-1802. doi:10.1152/jn.00680.2013

Miller, P. (1986). Gobiidae. In *Fishes of the North-Eastern Atlantic and Mediterranean*, Vol. 3 (ed. P. J. P. Whitehead, M. L. Bauchot, J. C. Hureau, J. Nielsen and E. Tortonese), pp. 1019-1085. Paris, France: United Nations Educational, Scientific and Cultural Organization.

Moles, A. and Norcross, B. L. (1995). Sediment preference in juvenile Pacific flatfishes. *Neth. J. Sea Res.* **34**, 177-182. doi:10.1016/0077-7579(95)90025-X

Moll, I., Kuhn, C. and Moll, R. (1995). Cytokeratin 20 is a general marker of cutaneous Merkel cells while certain neuronal proteins are absent. *J. Invest. Dermatol.* **104**, 910-915. doi:10.1111/1523-1747.ep12606183

Morley, J. W. and Goodwin, A. W. (1987). Sinusoidal movement of a grating across the monkey's fingerpad: temporal patterns of afferent fiber responses. *J. Neurosci.* **7**, 2181-2191. doi:10.1523/JNEUROSCI.07-07-02181.1987

Olsen, A. M. and Westneat, M. W. (2015). StereoMorph: an R package for the collection of 3D landmarks and curves using a stereo camera set-up. *Methods Ecol. Evol.* **6**, 351-356. doi:10.1111/2041-210X.12326

Phillips, J. R., Johansson, R. S. and Johnson, K. O. (1992). Responses of human mechanoreceptive afferents to embossed dot arrays scanned across fingerpad skin. *J. Neurosci.* **12**, 827-839. doi:10.1523/JNEUROSCI.12-03-00827.1992

Quiroga, R. Q., Nadasdy, Z. and Ben-Shaul, Y. (2004). Unsupervised spike detection and sorting with wavelets and superparamagnetic clustering. *Neural Comput.* **16**, 1661-1687. doi:10.1162/089976604774201631

Sawyer, E. K. and Catania, K. C. (2016). Somatosensory organ topography across the star of the star–nosed mole (*Condylura cristata*). *J. Comp. Neurol.* **524**, 917-929. doi:10.1002/cne.23943

Taft, N. K., Lauder, G. V. and Madden, P. G. A. (2008). Functional regionalization of the pectoral fin of the benthic longhorn sculpin during station holding and swimming. *J. Zool.* **276**, 159-167. doi:10.1111/j.1469-7998.2008.00472.x

Vega-Bermudez, F. and Johnson, K. O. (1999). SA1 and RA receptive fields, response variability, and population responses mapped with a probe array. *J. Neurophysiol.* **81**, 2701-2710. doi:10.1152/jn.1999.81.6.2701

Weber, A. I., Saal, H. P., Lieber, J. D., Cheng, J.-W., Manfredi, L. R., Dammann, J. F. and Bensmaia, S. J. (2013). Spatial and temporal codes mediate the tactile perception of natural textures. *Proc. Natl. Acad. Sci. USA* **110**, 17107-17112. doi:10.1073/pnas.1305509110

Wellnitz, S. A., Lesniak, D. R., Gerling, G. J. and Lumpkin, E. A. (2010). The regularity of sustained firing reveals two populations of slowly adapting touch receptors in mouse hairy skin. *J. Neurophysiol.* **103**, 3378-3388. doi:10.1152/jn.00810.2009

Westneat, M. W. (1996). Functional morphology of aquatic flight in fishes: kinematics, electromyography, and mechanical modeling of labriform locomotion. *Am. Zool.* **36**, 582-598. doi:10.1093/icb/36.6.582

Williams, R., , IV, Neubarth, N. and Hale, M. E. (2013). The function of fin rays as proprioceptive sensors in fish. *Nat. Commun.* **4**, 1729. doi:10.1038/ncomms2751

Yoshioka, T., Gibb, B., Dorsch, A. K., Hsiao, S. S. and Johnson, K. O. (2001). Neural coding mechanisms underlying perceived roughness of finely textured surfaces. *J. Neurosci.* **21**, 6905-6916. doi:10.1523/JNEUROSCI.21-17-06905.2001

Young, J. A. M., Marentette, J. R., Gross, C., McDonald, J. I., Verma, A., Marsh-Rollo, S. E., Macdonald, P. D. M., Earn, D. J. D. and Balshine, S. (2010). Demography and substrate affinity of the round goby (*Neogobius melanostomus*) in Hamilton Harbour. *J. G. Lakes Res.* **36**, 115-122. doi:10.1016/j.jglr.2009.11.001
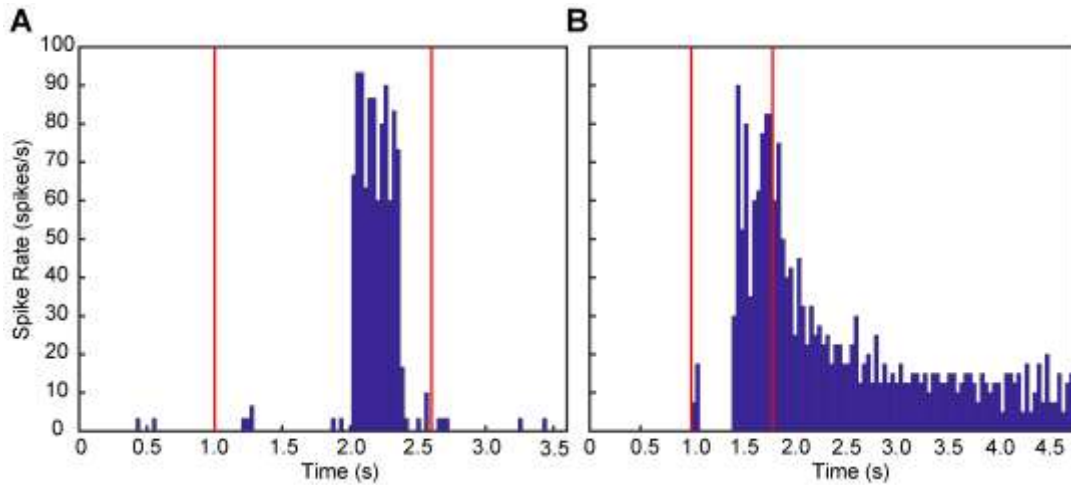
Fig S1. Temporal response profiles to a proximodistal brushing stimuli. (A) Poststimulus time histogram (PSTH, bin width 30 ms) from a representative afferent showing the mean firing rate across 10 trials to a proximodistal brushing stimuli moving across the fin surface at 5 mm/sec. The red vertical lines indicate the onset and offset of the stimulus. The temporal response profiles of units used in the analysis of receptive field size typically consisted of a prolonged period of sustained activity with a high spike rate bordered by periods of sparse or no firing. (B) PSTH (10 trials, bin width 40 ms) from a representative afferent that continued to fire well after the stimulus offset indicative of a slowly adapting response to the sustained indentation of the probe. The response is characterized by a sharp decrease in firing rate shortly after stimulus offset (rightmost red vertical line) followed by an extended period of tonic firing. When averaged across afferents (n = 4) and trials, the spike rate (spikes/s) during the period of prolonged indentation was 13.63 ± 3.71 (mean $\pm$ s.d.).
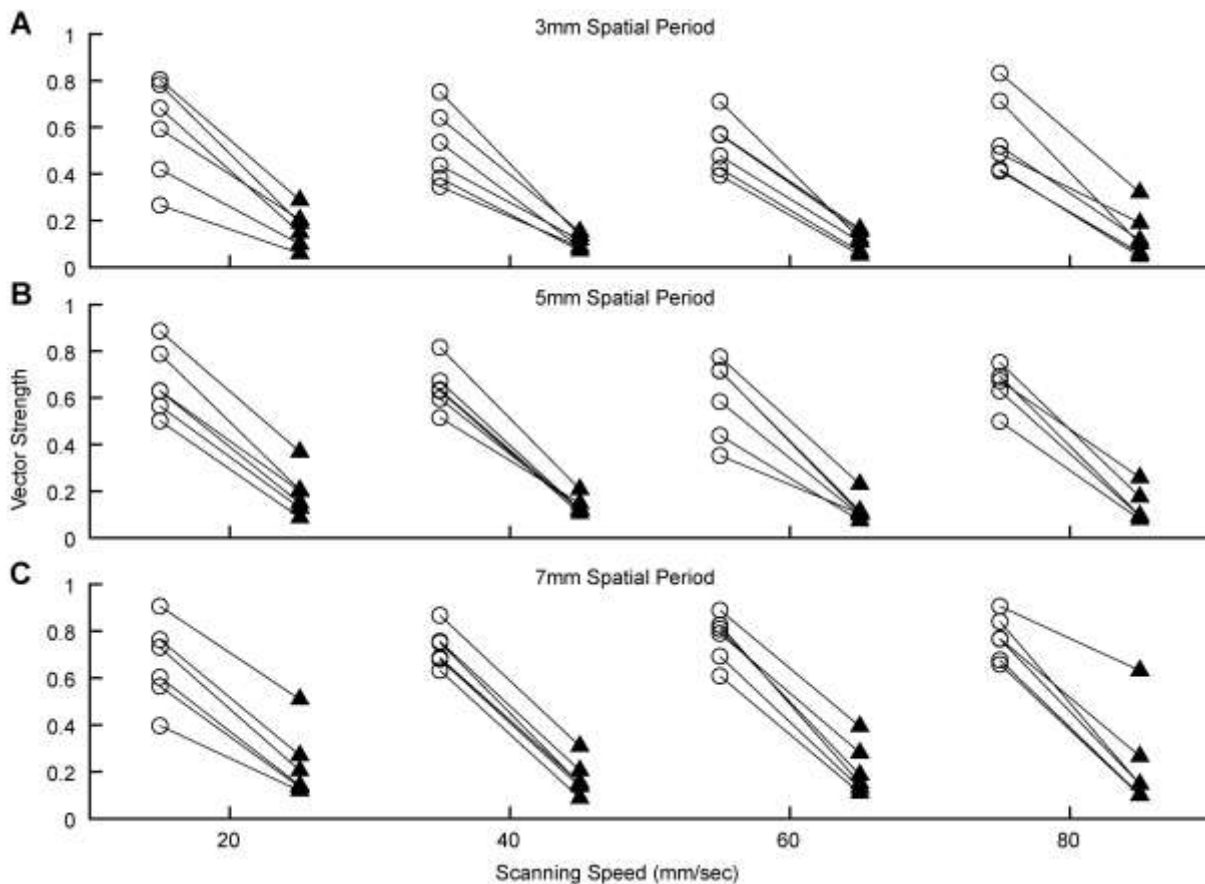
Fig S2. Comparison of vector strength between the observed and simulated afferent responses to the spatial period of coarse gratings. Vector strength, a measure of phase locking between a periodic stimulus and a neural response, ranges from 0 for uniform firing across all phases of the stimulus to 1 for perfectly synchronized firing at only one phase location relative to each passing stimulus. Each row of plots shows the vector strength of the observed and simulated response for each afferent (n = 6) to gratings with a (A) 3 mm, (B) 5 mm, or (C) 7 mm spatial period scanned across the fin at 20, 40, 60, or 80 mm/s. Open circles mark the observed mean (n = 5 trials) vector strength value for a given combination of grating spatial period and scanning speed. Filled triangles mark the simulated mean (n = 5 trials) vector strength value expected by chance if there was no cyclic entrainment (see Materials and Methods). Lines connect data points from a given afferent. Vector strength values for each combination of spatial period and scanning speed were significantly higher than expected by chance (P < 0.001). The high degree of phase locking provides precise information on the temporal frequency on coarse gratings independent of the grating spatial period or scanning speed.

Table S1. Summary data associated with response properties to tactile motion for each afferent (n = 8) include in the analysis of receptive field size. All values are presented as the mean ± standard deviation.

Afferent ID	Scanning Speed (mm/s)	Stimulus Evoked Spikes	Duration of Stimuls Evoked Activity (s)	Spike Rate (spikes/s)	Receptive Field Size (mm)
1	5	40.3 ± 2.54	0.660 ± 0.079	61.80 ± 8.07	3.30 ± 0.393
	10	28.5 ± 2.51	0.365 ± 0.027	78.23 ± 7.38	3.65 ± 0.270
	20	14.7 ± 2.16	0.214 ± 0.035	69.72 ± 11.62	4.27 ± 0.696
2	5	29.3 ± 2.50	0.434 ± 0.120	70.19 ± 11.72	2.17 ± 0.549
	10	15.7 ± 1.70	0.270 ± 0.041	59.01 ± 7.85	2.70 ± 0.411
	20	7.1 ± 1.37	0.100 ± 0.052	80.62 ± 23.94	2.00 ± 1.034
3	5	33.6 ± 5.80	1.088 ± 0.062	30.84 ± 4.69	5.44 ± 0.311
	10	19.0 ± 3.16	0.515 ± 0.055	37.22 ± 6.69	5.15 ± 0.554
	20	10.2 ± 1.40	0.224 ± 0.027	45.72 ± 5.22	4.48 ± 0.538
4	5	38.4 ± 2.32	0.831 ± 0.029	46.26 ± 3.16	4.15 ± 0.147
	10	19.3 ± 1.34	0.395 ± 0.027	49.02 ± 3.75	3.95 ± 0.276
	20	13.0 ± 1.41	0.174 ± 0.031	76.02 ± 9.12	3.48 ± 0.622
5	5	52.1 ± 5.51	0.872 ± 0.027	59.68 ± 5.23	4.36 ± 0.136
	10	23.7 ± 2.31	0.469 ± 0.011	50.51 ± 4.40	4.69 ± 0.112
	20	14.4 ± 1.51	0.231 ± 0.011	62.26 ± 6.07	4.63 ± 0.234
6	5	44.5 ± 2.80	0.798 ± 0.016	55.76 ± 3.42	3.99 ± 0.079
	10	18.9 ± 2.33	0.403 ± 0.031	47.03 ± 5.43	4.03 ± 0.314
	20	14.0 ± 1.33	0.242 ± 0.024	58.21 ± 7.33	4.85 ± 0.485
7	5	28.1 ± 3.28	0.525 ± 0.020	53.59 ± 6.59	2.63 ± 0.102
	10	15.8 ± 2.94	0.264 ± 0.079	61.90 ± 12.19	2.64 ± 0.788
	20	11.7 ± 1.89	0.183 ± 0.062	68.08 ± 15.85	3.67 ± 1.243
8	5	45.9 ± 7.36	0.824 ± 0.012	55.67 ± 8.95	4.12 ± 0.061
	10	35.4 ± 5.76	0.408 ± 0.012	86.79 ± 13.53	4.08 ± 0.127
	20	10.7 ± 1.70	0.208 ± 0.032	51.95 ± 8.20	4.16 ± 0.648